Problem 1: Cardiovascular events associated with oral and IV-administered antibacterial agents*

Daniel Beavers[†], Abhishek Bhattacharya[‡], Matthew Causley[§],
Juanjuan Chai[¶], Kathleen Holm[‖], Nate Wanner[**]

Problem Presenter:
Jeffrey D. Wetherington
Glaxo SmithKline

Faculty Mentors:
Grace M. Kepler, H. T. Banks, and Ariel Cintrón-Arias
Center for Research in Scientific Computation
Center for Quantitative Sciences in Biomedicine
North Carolina State University

July 29, 2008

Abstract

A new antimicrobial pharmaceutical compound being developed appears to be effective against methicillin-resistant Staphylococcus aureus infection in pre-clinical experiments. At high doses, the compound appears to induce premature ventricular contractions in animal models, creating concern about the safety of the compound and whether the timing of the dosage can ameliorate the likelihood of adverse events. We develop a compartmental model to simulate the pharmacokinetics of the drug from injection into the bloodstream until absorption into the heart via the coronary artery. We attempt to develop a dosing strategy to maximize the absorption into the lung while minimizing the dosage that arrives at the heart based on animal models and a previously published study on the pharmacokinetics of erythromycin. We explore the mathematical properties of our model and propose future considerations for improvement of the current model and for the development of a statistical model for estimation of the parameters based on empirical data.

*Research conducted through SAMSI and CRSC
[†]Baylor University
[‡]University of Arizona
[§]New Jersey Institute of Technology
[¶]Indiana University
[‖]North Carolina State University
[**]North Carolina State University

Contents

1 Introduction

A new antibacterial compound is in development at Glaxo SmithKline to cure pneumonia and methicillin-resistant Staphylococcus aureus (MRSA) infections. This compound can be effective at either of two bacterial sites, giving it lower probability of resistance. In vitro experiments have shown that this drug successfully kills the bacteria, with probability of resistance less than 10^{-9} [21]. Pre-clinical trials in beagles have shown that this drug causes arrhythmias (premature ventricular contractions: PVCs) for some beagles when the drug is administered intravenously (IV). Arrhythmias do not occur when the compound is administered orally, but this may be explained by a lower overall dose. Arrhythmias occurred more frequently in beagles with a higher overall dose. This is a serious concern since PVCs pose a heart attack risk.

Although the mechanism behind the drug-related arrhythmias is unknown, our hypothesis is that accumulation of the drug in the cardiac tissue, mostly from the first pass of the drug through the body, is one of the main causes. We develop a mathematical-pharmacokinetic model for concentration of the IV drug at different sensor locations within the body. The main goal of this model is to predict the accumulation of the drug in the cardiac tissue from its first pass through the heart. With this model we hope to find an optimal dosing strategy that would maximize accumulation of the drug in the lungs, in order to treat pneumonia, while minimizing accumulation in the cardiac tissue.

We developed a pharmacokinetic model to address the goals mentioned above. This model is based on physiological events that occur as the drug is given intravenously, as it flows through the blood, and through its first passage into the heart. The compartments in the model reflect physical locations of sensors that measure drug concentration. This initial model attempt was adapted from the work of Upton [14]. This model predicts the concentration of the drug in the lung, the target organ for the treatment of pneumonia, and cardiac tissue. We also show how we can use this model to predict the arrhythmia response from the concentration of the drug in the cardiac tissue.

It is also necessary to have biologically relevant estimates for the parameters of the model. In the presence of data at the sensory locations, and measurements for fixed parameters in the model, we could fit the model to the data to best estimate the controlled parameters, such as dose amount. However, due to the proprietary nature of this research much of this data was unavailable. Baseline values of parameters were obtained from the literature, with the majority being sheep parameter values [14].

This report is organized as follows: In Section 2 we descibe the pharmacokinetic model. In Section 3 we report and discuss numerical simulations of the model. In Section 4 we analyze the sensitivity of the concentration solutions to the parameters, and conduct an optimization for dose time, T. In Section 5, we consider another dosing strategy. In Section 6, we propose a method for connecting this model to the observed arrhymias effects. In Section 7, we examine this model as it relates to statistics. In Section 8, we make conclusions, discuss some issues with this model, and describe our future work.

2 Methodology

The cardiovascular system is a complex network of blood vessels that provides the cells of the body with the nutrients they need [13]. To model how the drug is distributed to the lungs and heart, an approach taken by Upton et. al will be used [14]-[19]; the general framework to model the first-pass effects of a drug used by Upton et. al can be seen in Fig. 1. A simplifcation of this system can be seen in Fig. 2(a). Here the target organ would be the heart and the target organ effects would be arrhythmias. The framework shown in the figure was adapted for this problem to include a compartment for the lung. For modeling purposes, we will consider injection of the drug into a vein. From here, the blood containing the drug will pass through the right side of the heart, the pulmonary artery, the lungs, the pulmonary vein, the left side of the heart, and then into the aorta. The coronary artery is a vessel that branches off from the aorta near its base, and its function is to supply the tissue of the heart with the oxygen and nutrients it needs [13]. Since we are most concered with the affects of the drug during its first pass through the system, we will not consider the affects of systemic circulation such as metabolism in the liver.

In compartmental modeling, a compartment can represent a physiological subdivision of a system throughout which the behavior of a substance is uniform [5]. The compartmental model analyzed in this paper can be seen in Fig. 2(b). We will consider the concentration of the drug in the pulmonary artery, the aortic arch, the lungs,

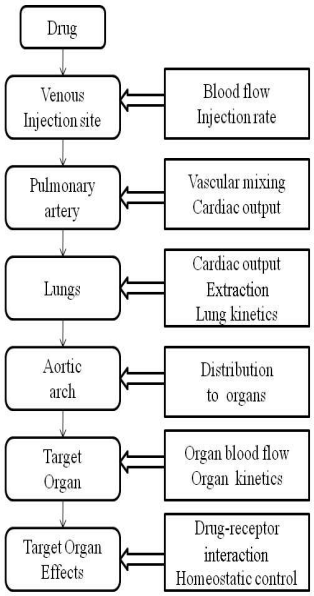

Figure 1: An overview of the process affecting the first pass drug concentration. The left panels indicate the sites of various sensor locations within the body, the right ones indicate the most important aspects of the process.

and the coronary artery. An important assumption to be made in the model is that the drug will not be absorbed into the heart as it passes through the organ. In other words, the drug will only be absorbed into the heart once it reaches the tissue via the coronary artery. In order to model mass transport between the compartments, we will also assume the compartments have constant volume and are well-mixed.

2.1 Model

The model is broken into compartments where the drug concentration can be calculated separately as it passes through the system. They are set up to track the fate of the drug through the pulmonary artery, lung, aortic arch, and coronary sinus. Initialization of the model is obtained by describing the nature of the IV administration of the drug, and this appears explicitly as a term in the first compartment included in the model.

2.1.1 Pulmonary artery

An amount D of the drug is assumed to be injected at a constant rate over given time T. The resulting piecewise constant distribution, commonly referred to as a square wave, represents the drug concentration in the blood immediately downstream of the injection site. After injection, the square wave travels from the injection site to the pulmonary artery, with two factors influencing its shape in transit. First, it is diluted with other venous blood, until the drug has been diluted with the entire cardiac output (Q_T) as it passes through the pulmonary artery. We ignore the time taken to travel from the injection site to the pulmonary artery, so that the unmixed concentration (C_U) is given by the following equation

$$C_U(t) = \begin{cases} \frac{Df}{TQ_T} & \text{if } 0 \leq t \leq T \\ 0 & \text{if } t > T \end{cases} \tag{2.1}$$

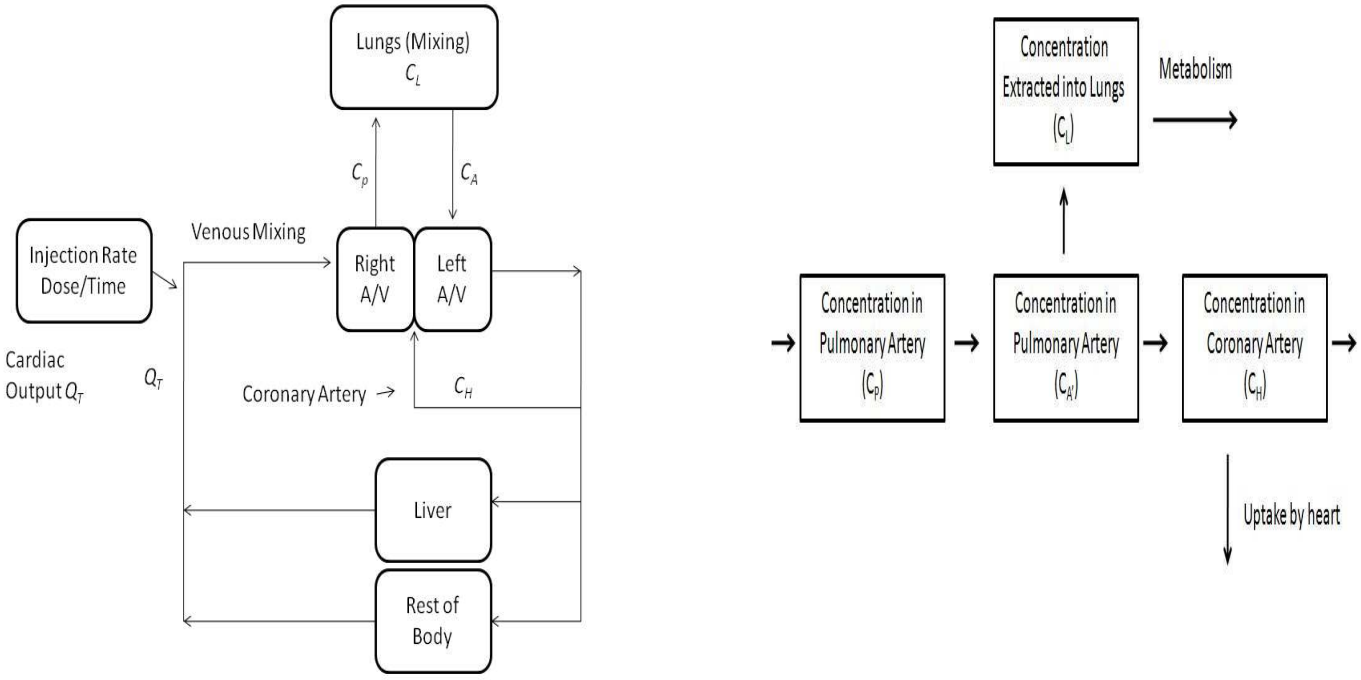

Figure 2: (a) Simplification of circulatory system and (b) representation of model

Second, the square wave will be modified by factors such as dispersion during transit along the vessel, plasma binding and dynamics of the mixing process. For simplicity, we assume the plasma binding affects a uniform decrease in the amount of the delivered drug to the pulmonary artery, which is equivalent to decreasing the dose by a factor f. To represent the concentration in the pulmonary artery, we will use a common method known as a single well-stirred compartment model or a flow-limited model [19]. The derviation below is modified from Upton[19]. If we first take the target compartment to neither extract nor metabolize any of the drug, then we can apply the law of conservation of mass. Thus the total mass of drug in the compartment will be the difference in the mass entering via the incoming blood and that leaving via the outcoming blood. This is true over any given time interval. Therefore, flux of the drug mass in the pulmonary artery will be the difference of the entering and exiting flux,

$$\text{(Net rate in pulmonary artery)} = \text{(Rate in)} - \text{(Rate out)}. \tag{2.2}$$

However, the volume of blood in the artery is fixed. If we further assume a constant flow of blood volume per unit time Q_T,

$$Q_T C_U - Q_T C_{out} = Q_T(C_U - C_{out}) \sim [mg/min], \tag{2.3}$$

where C_{out} denotes the concentration of the drug leaving the pulmonary artery. Here we use $\sim [\cdot]$ to denote the units. Notice that the mass of the drug in the pulmonary artery is equal to the concentration (C_P) multiplied by the hypothetical mixing volume (V_M),

$$V_M C_P \sim [L \cdot mg/L = mg]. \tag{2.4}$$

It is the concentration of drug in the pulmonary artery rather than this mixing volume that will change with time (say from time t_1 to t_2). So the rate of change of the mass in the pulmonary is

$$V_M \frac{C_P(t_2) - C_P(t_1)}{t_2 - t_1} \sim [mg/min]. \tag{2.5}$$

By taking a limit as $(t_2 - t_1) \to 0$, we can combine the above to obtain

$$V_M \frac{dC_P}{dt} = Q_T \cdot (C_U - C_{out}). \tag{2.6}$$

By considering a "well stirred" compartment [14], we take the exiting concentration to be equivalent to the pulmonary concentration. This is the "pulmonary equilibrium", and dividing the volume V_M gives the final equation

$$\frac{dC_P}{dt} = \frac{Q_T}{V_M} (C_U - C_P). \tag{2.7}$$

This is the first differential equation in the model. The same idea will be used to obtain the equations for other organs later.

2.1.2 Lungs & Aortic arch

In addition to the terms in the equation in the pulmonary artery, the equation for the lung will have two additional terms. These additions will account for extraction of the drug into the tissue of the lung and metabolism of the drug. It is assumed that these events happen sequentially. The first portion of the equation then is

$$\frac{dC_{A'}}{dt} = \frac{Q_T}{V_L} (C_P - C_{A'}), \tag{2.8}$$

where $C_{A'}$ can be thought of as the concentration in the lung compartment if no extraction or metabolism exists, V_L denotes the apparent volume of the lung, C_P is the concentration leaving the pulmonary artery, which is in the same form as (2.7), and C_A will be used to denote the concentration of the drug in the venous blood emerging from the lung. An extraction constant E_L will account for the fraction $(0 < E_L < 1)$ of the mass of the drug absorbed into of the lungs; assuming constant volume of the aortic arch, this will give

$$C_A = C_{A'}(1 - E_L). \tag{2.9}$$

Although it makes more sense to think of a mass being extracted rather than a concentration, under the assumption of constant volume in the lung compartment, we can define C_L to be the concentration of the drug extracted into the lungs. To model the metabolism of the drug we consider the biological processes due to the enzymes

$$E + S \underset{k_{-1}}{\overset{k_1}{\rightleftarrows}} ES \xrightarrow{k_2} E + P,$$

where E denotes the concentration of the enzyme, S denotes the drug concentration, while ES is the reaction complex, and P denotes the product.
By the Michaelis - Menten equation [20], we have the rate of the metabolism of the drug equals

$$\frac{dP}{dt} = V_0 \frac{C_L}{K_m + C_L}, \tag{2.10}$$

in which V_0 denotes the maximum velocity of the enzyme, and K_m is the Michaelis constant which is defined as

$$K_m = \frac{k_{-1} + k_2}{k_1}. \tag{2.11}$$

We finally, combine (2.8) with (2.10) to form the equation for the drug concentration extracted to the lungs (C_L)

$$\frac{dC_L}{dt} = \frac{dC_{A'}}{dt} E_L - \frac{V_0 C_L}{K_m + C_L} = \frac{Q_T E_L}{V_L} (C_P - C_{A'}) - \frac{V_0 C_L}{K_m + C_L}.$$

Table 1: Time-dependent state variables

State variable	Definition
$C_{A'}$	Concentration of drug in aortic arch, with no extraction in the lung
C_A	Concentration of drug in aortic arch
C_H	Concentration of drug in coronary artery
C_L	Concentration of drug extracted to the lung
C_p	Concentration of drug in pulmonary artery

2.1.3 Target Organ

Emerging from the lungs in venous blood, the drug is distributed to other organs of the body; in our model, the only target organ considered is the coronary sinus, a large vessel in the heart. The coronary sinus (or heart) concentration is modelled with a single compartment with a small first-order extraction term with constant rate k. Letting C_H denote the drug concentration in the coronary artery, Q_H denote the blood flow in the target organ, and V_H denote the apparent volume of the heart, then the equation is given by

$$\frac{dC_H}{dt} = \frac{Q_H}{V_H}((1-E_L)C_{A'} - C_H) - \frac{k}{V_H}C_H. \tag{2.13}$$

2.1.4 Model Equations

In summary, our system of equations is

$$\begin{aligned}
\frac{dC_P}{dt} &= \frac{Q_T}{V_M}(C_U(t) - C_P(t)) && (2.14)\\
\frac{dC_{A'}}{dt} &= \frac{Q_T}{V_L}(C_P(t) - C_{A'}(t)) && (2.15)\\
\frac{dC_L}{dt} &= \frac{Q_T E_L}{V_L}(C_P(t) - C_{A'}(t)) - \frac{V_0 C_L(t)}{K_m + C_L(t)} && (2.16)\\
\frac{dC_H}{dt} &= \frac{Q_H}{V_H}((1-E_L)C_{A'}(t) - C_H(t)) - \frac{k}{V_H}C_H(t) && (2.17)\\
C_A(t) &= C_{A'}(t)(1-E_L) && (2.18)\\
C_P(t_0) &= 0 && (2.19)\\
C_{A'}(t_0) &= 0 && (2.20)\\
C_L(t_0) &= 0 && (2.21)\\
C_H(t_0) &= 0 && (2.22)
\end{aligned}$$

$$C_U(t) = \begin{cases} \frac{Df}{TQ_T} & \text{if } 0 \le t \le T \\ 0 & \text{if } t > T \end{cases} \tag{2.23}$$

Tables 1 and 2 describe the state variables and the parameter values we used.
We may also define the vector of parameters in the equations by

$$\theta = (Q_T, V_M, V_L, E_L, Q_H, V_H, k, D, T, V_0, K_m, f) \tag{2.24}$$

Table 2: Parameter values

Parameter	Definition	Baseline value	Unit	Context	Reference
D	Total dose amount	100	mg		[14]
E_L	First pass extraction by the lung	0.32	$0 < E_L < 1$	Sheep	[14]
f	Non-plasma bound proportion	0.6	$0 < f < 1$	Erythromycin	[22]
k_H	First order loss rate constant from the heart	0.062	Liter/min	Sheep	[14]
k_M	Concentration constant	100	mg/Liter		-
Q_H	Flow rate through coronary artery	0.122	Liter/min	Sheep	[14]
Q_T	Cardiac output (flow rate)	5.6	Liter/min	Sheep	[14], [15]
T	Dose delivery time	1	min		-
V_0	Maximum metabolism rate in the lung	1	mg/Liter/min		-
V_H	Volume of the heart	0.45	Liter	Sheep	[14]
V_L	Volume of the lung	1.06	Liter	Sheep	[14]
V_M	Volume of the venous mixing compartment	0.255	Liter	Sheep	[14], [15]

and the state variable vector, for a given parameter vector θ and time t, as

$$x(t;\theta) = \begin{bmatrix} C_P(t;\theta) \\ C_{A'}(t;\theta) \\ C_L(t;\theta) \\ C_H(t;\theta), \end{bmatrix} \tag{2.25}$$

which allows us to write (2.14)-(2.17) in the compact form as [1],

$$\frac{dx}{dt} = g(x(t;\theta);\theta), \tag{2.26}$$

where the vector function g is defined by the right-side of equations (2.14)–(2.17). This form of the equations will be used in the sensitivity analsyis.

3 Numerical Results

While the goal is to determine optimal dosing strategy, the sensitivity analysis indicated that varying dose administration time T was more important than varying dose amount D. Therefore a dose amount of 100 mg of the drug was administered in a square wave distribution over a delivery time of 30 and 60 seconds respectively. Equations (2.14)-(2.22) were solved in MATLAB using the ode15s solver to ensure resolution of any sharp wave fronts created by the corners of the initial dose distribution. The chosen parameters are listed in Table 2, and plots of the solutions for C_P, C_L, C_A and C_H were obtained as shown in Fig. 3. Note that while the plot of C_A is the correct concentration amount for the aortic arch, it is not the same concentration as calculated by equation (2.16), which is for $C_{A'}$; however these two quantities are linearly related by $C_A = (1 - E_L)C_{A'}$.

Varying the amount of the dose was found to only effect the relative heights of each concentration distribution. Therefore, doubling the dose amount would double the concentrations in each respective area. A few prominent features of the effects of varying T can be seen by viewing the different compartments. In Fig. 3 which shows C_P the dose travelling through the pulmonary artery en route to the lung, the right side of the peak still contains the sharp discontinuity created by the square wave, but it is beginning to diffuse. The peak concentration can be seen to increase from the T=60 seconds (solid) to the T=30 seconds (dashed). This should be intuitive: since the same dose amount is being injected, the bolus will be more concentrated, with a shorter delivery time, thus resulting in a higher peak concentration. The drug will then leave the pulmonary artery, and enter the lung C_L. The concentration extracted to the lung is noticeably smaller than that in the pulmonary artery and the steep decline in drug concentration at the right side is beginning to diffuse, forming a tail of residual concentration. The same can be seen in C_A, the concentration of the aortic arch, although to a more pronounced degree than in the lung. This behavior continues until in the heart the original shape of the wave form has diffused and any sharp changes in concentration have now vanished. The peak concentration in the heart is an order of magnitude

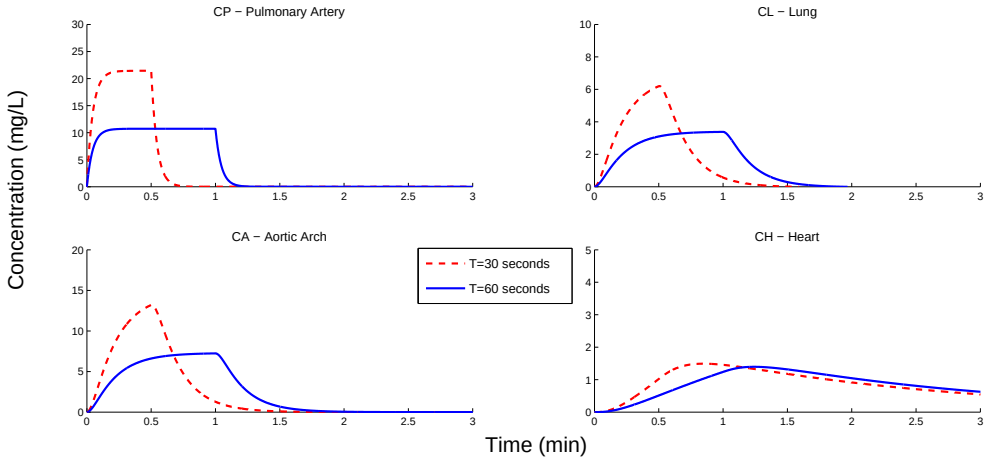

Figure 3: Comparisons of 30 and 60 second simulations.

less than that which is in the pulmonary artery. It is noteworthy that while varying T greatly changes the peak concentration of C_L, the corresponding peaks for C_H are not affected.

4 Sensitivity of Concentration Solutions and Optimization to Parameters

Sensitivities of the state variables (C_P,$C_{A'}$,C_L,C_H) to the parameters $\theta = (Q_T, V_M, V_L, E_L, Q_H, V_H, k, D, T, V_0, K_M)$ were calculated. Our sensitivity analysis is described below:

Differentiating with respect to θ —in both sides of (2.26)— one obtains,

$$\frac{\partial}{\partial\theta}\frac{dx}{dt} = \frac{\partial}{\partial\theta}g(x(t;\theta);\theta), \tag{4.1}$$

which implies

$$\frac{d}{dt}\frac{\partial x}{\partial\theta} = \frac{\partial g}{\partial x}\frac{\partial x}{\partial\theta} + \frac{\partial g}{\partial\theta}. \tag{4.2}$$

Numerical solutions of the sensitivity functions, $\partial x/\partial\theta_i$, are calculated by solving (2.26) and (4.2) simultaneously using $\theta_i = \hat{\theta}_i$, where $\hat{\theta}_i$ denotes a known value for the ith parameter.

Relative sensitivities can be found using solutions $x(t;\theta)$, $\partial x(t;\theta)/\partial\theta$ and parameter estimate $\theta = \hat{\theta}$, to obtain.

$$s_{\theta_i}(t) = \frac{\hat{\theta}_i}{x(t;\theta)}\frac{\partial x(t;\theta)}{\partial\theta_i}, \qquad \text{for } \; i : 1 \le i \le p. \tag{4.3}$$

Sensitivity functions and relative sensitivity functions were solved for numerically using baseline values from Table 2. The results of of this analysis can be seen in Fig. 4 and Fig. 5.

As can be seen in Fig. 4, the sensitivity of concentration on the parameters depends on the time interval. The dose time T was set to be 1 minute. This had an effect on the important time intervals for the sensitivities. Positive sensitivity values indicate that the concentration is sensitive to increasing in response to increasing variation in the parameter in that time interval. Concentration $C_P(t;\theta)$ is most sensitive to V_M when $t \approx 0$ and when $t \approx 1$. When $t < 1$, $C_p(t;\theta)$ is sensitive to decreasing in response to increasing variation in the parameter T. Concentration $C_{A'}(t;\theta)$ is most sensitive to parameters T and V_L for $t < 2$. The sensitivity of concentration $C_L(t;\theta)$ to E_L, T, and V_L is greater when $t < 1.5$. The concentration $C_H(t;\theta)$ is most sensitive to Q_H when $t < 4$, and is sensitive (to a lesser extent) to k, V_H, and E_L around $t \approx 1$.

Since the parameters in this model vary greatly in magnitude, it is also important to consider the relative sensitivity functions. Figure 5 shows the relative sensitivity of each concentration to the parameters. The

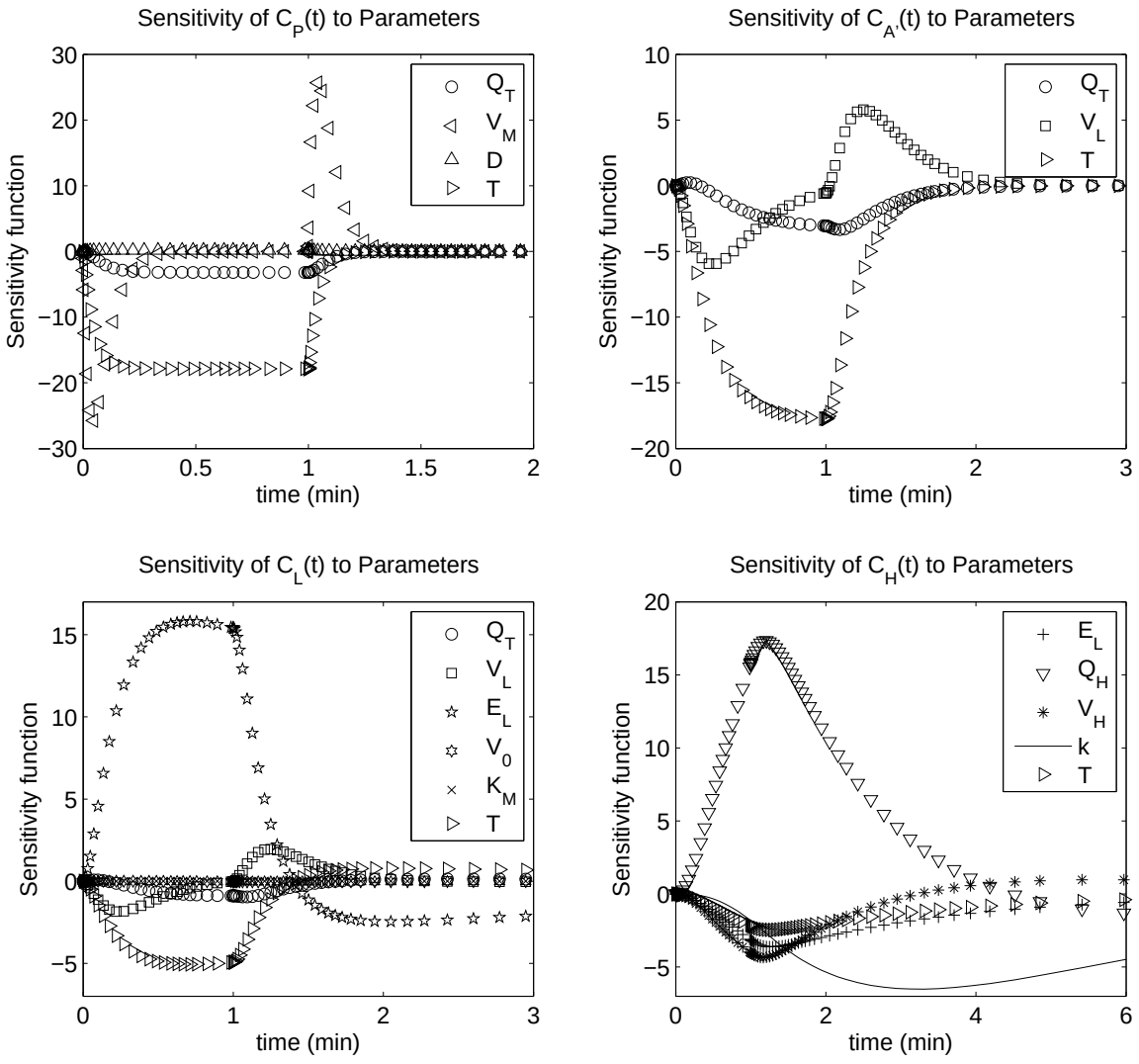

Figure 4: Sensitivity functions for all parameters.

concentration $C_P(t;\theta)$ is not relatively sensitive to any parameters for $t < 1$, but it is sensitive to V_M and Q_T when $t > 2$. Concentration $C_{A'}(t;\theta)$ is relatively sensitive to V_L and Q_T when $t > 2$. The concentration $C_L(t;\theta)$ is relatively sensitive to Q_T, V_L, K_M, and V_0 only at time $t \approx 1.5$. The relative sensitivities of $C_H(t;\theta)$ change over time, being most relatively sensitive to V_H (highest relative sensitivity), then Q_H and T.

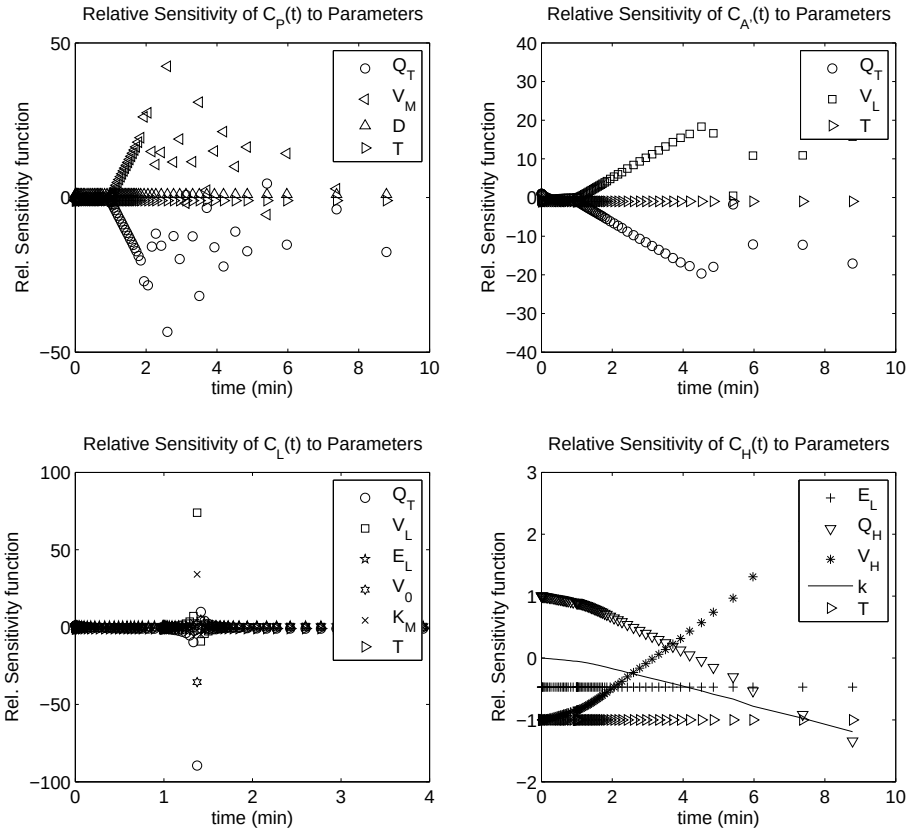

Figure 5: Relative sensitivity functions for all parameters.

These sensitivities arise from our system of equations describing the biological system. At certain time points it is more important to take the measurement if the concentration solutions are more sensitive at the point. If possible, this should be taken into consideration for experimental design to help improve the model. For example, if the concentration in the coronary sinus (heart), C_H, is the main objective, then experiments that could suggest more accurate values of the parameters Q_H and V_H would be necessary for more informative results, since C_H is the most sensitive to those parameters.

4.1 Sensitivity of optimization cost function to parameters

We also examined sensitivities for an optimization problem defined as

$$\max_{\theta} L(\theta) = \max_{\theta} \frac{L_1(\theta)}{L_2(\theta)}, \tag{4.4}$$

where

$$L_1(\theta) = \int_{t_0}^{t_n} C_L(t;\theta)dt, \tag{4.5}$$

$$L_2(\theta) = \int_{t_0}^{t_n} C_H(t;\theta)dt, \tag{4.6}$$

[h!] assuming the time points are $t_0, t_1, \ldots, t_n$. The maximum of this cost function will maximize the concentration of the drug extracted into the lung, while minimizing the concentration of the blood in the coronary sinus. The result of this optimization will be a set of parameters, including the parameters that specify a dosing strategy, that accomplish this. However, optimization schemes need initial parameter estimates. The sensitivity analysis informs us as to which initial parameter estimates the optimization results are most sensitive to. Using equation 4.3, we were able to calculate the relative sensitivities of the cost function $L(\theta)$ to the parameters. The results are presented below in Table 3. The values in the table are ranked from most negatively sensitive (value of cost function more sensitive to decreasing) to most positive. From this we can see that this optimization scheme is most sensitive to E_L, K_M, and V_0.

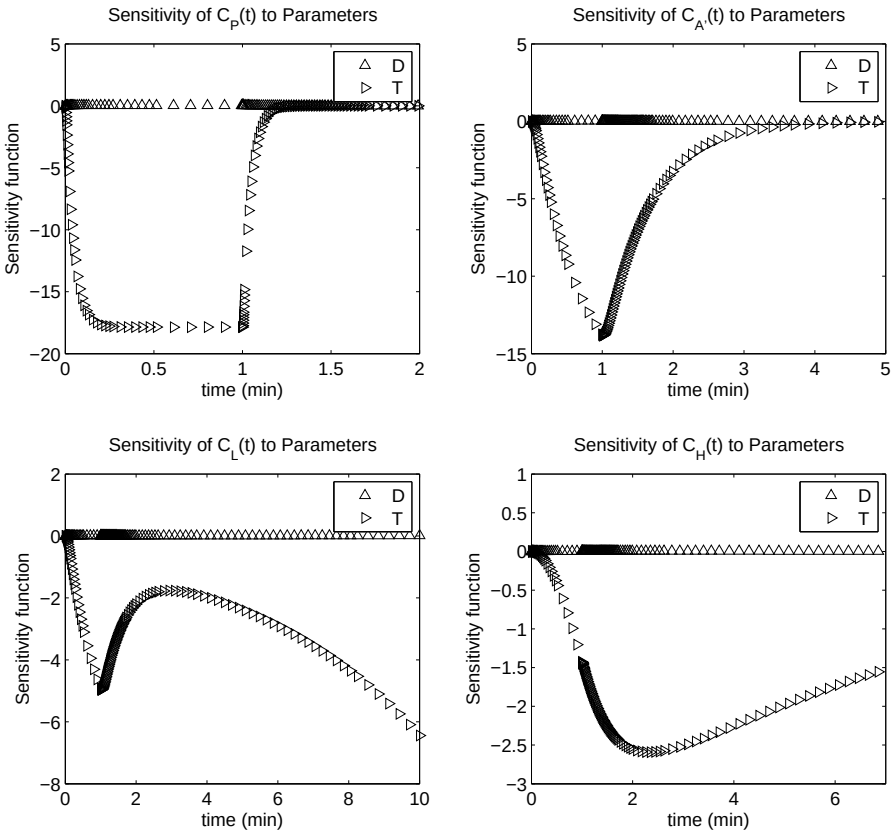

Figure 6: Sensitivity functions for parameters D and T, only.

To illustrate the usefulness of this sensitivity analysis, we conducted the optimization. The optimatization algorithm minimizes the cost function $L(\theta)$, so we used the multiplicative inverse. We also squared it to give the optimization algorithm better convergence properties. The implemented optimization problem is

$$\min_{\theta} \left[\frac{L_2(\theta)}{L_1(\theta)}\right]^2 \tag{4.7}$$

Table 3: Relative sensitivities of parameters to cost function $L(\theta) = \frac{L_1(\theta)}{L_2(\theta)}$.

Relative Sensitivity	Value
$\frac{E_L}{L}\frac{\partial L}{\partial E_L}$	-1.6344
$\frac{K_m}{L}\frac{\partial L}{\partial K_m}$	-1.3274
$\frac{k}{L}\frac{\partial L}{\partial k}$	-0.3072
$\frac{D}{L}\frac{\partial L}{\partial D}$	-0.1638
$\frac{V_H}{L}\frac{\partial L}{\partial V_H}$	-0.0882
$\frac{V_M}{L}\frac{\partial L}{\partial V_M}$	-0.0040
$\frac{V_L}{L}\frac{\partial L}{\partial V_L}$	0.0078
$\frac{Q_T}{L}\frac{\partial L}{\partial Q_T}$	0.1600
$\frac{T}{L}\frac{\partial L}{\partial T}$	0.1638
$\frac{Q_H}{L}\frac{\partial L}{\partial Q_H}$	0.3954
$\frac{V_0}{L}\frac{\partial L}{\partial V_0}$	1.4913

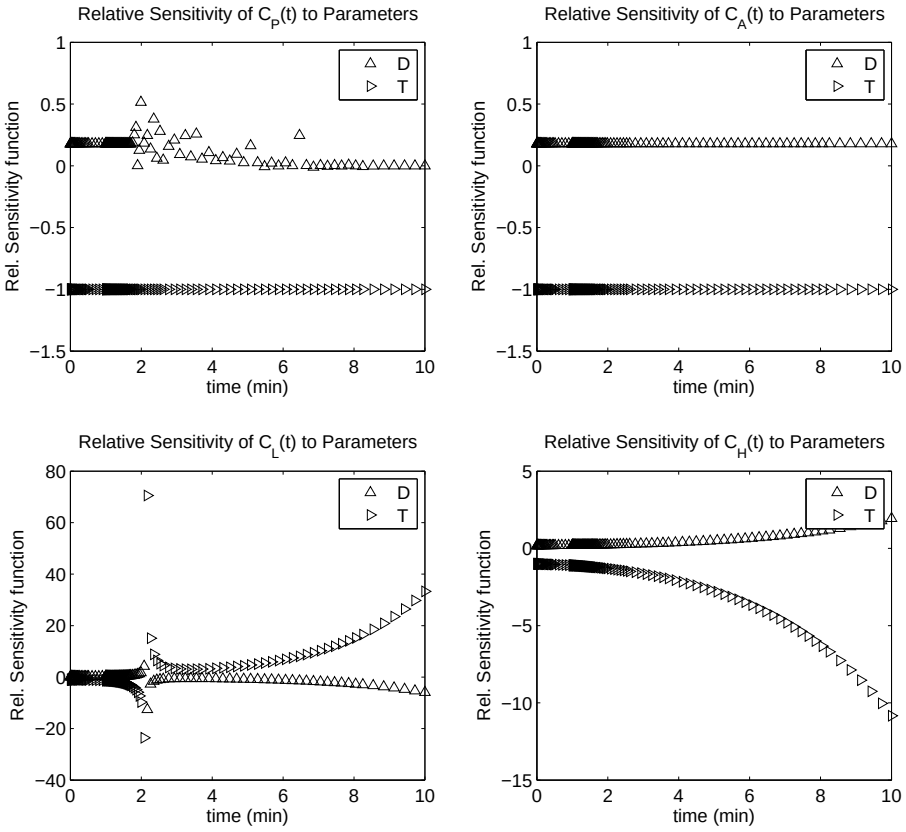

Figure 7: Relative sensitivity functions for parameters D and T, only.

Table 4: Cost function $L(\theta) = [L_2(\theta)/L_1(\theta)]^2$.

Parameter	Initial guess	Optimal value
Q_T	5.628×10^{0}	7.245×10^{0}
V_M	2.563×10^{-1}	2.805×10^{-1}
V_L	1.065×10^{0}	1.370×10^{0}
E_L	3.216×10^{-1}	1.848×10^{-21}
Q_H	1.226×10^{-1}	1.123×10^{-1}
V_H	4.522×10^{-1}	4.696×10^{-1}
k	6.231×10^{-2}	6.081×10^{-2}
D	1.005×10^{2}	1.023×10^{2}
T	1.005×10^{0}	9.473×10^{-1}
V_0	2.010×10^{1}	2.951×10^{1}
K_M	1.005×10^{2}	7.851×10^{1}
Minimum value of cost function $L(\hat{\theta})$=2.873×10^{-45}		

Table 5: Relative sentivities of only two parameters to cost Function $L(\theta) = \frac{L_1(\theta)}{L_2(\theta)}$.

Relative Sensitivity	Value
$\frac{D}{L}\frac{\partial L}{\partial D}$	-4.8809
$\frac{T}{L}\frac{\partial L}{\partial T}$	27.3326

Table 6: Cost function $L(\theta) = [L_2(\theta)/L_1(\theta)]^2$.

Parameter	Initial guess	Optimal value
D	1.005×10^{2}	1.518×10^{1}
T	1.005×10^{0}	6.285×10^{-2}
Minimum value of cost function $L(\hat{\theta})$=9.005×10^{-20}		

The results of the optimatization are in Table 4 . The initial parameter estimates and the value of the parameter that the optimization converged to are also given. Upon examining the difference in magnitude between the initial estimate and the optimized value we see that E_L differs the most and then K_M to a lesser extent. This corresponds with the relative sensitivity value we found, since both E_L and K_M had the two most negative relative sensitivity values.

4.2 Sensitivity of state variables to D and T

Considering the parameters of this model, total dose D and dose time T are the parameters we can adjust. The other parameters are specific to the drug and the patient's physiology. We calculated the sensitivity again for D and T, but this time holding all other parameters fixed. Using equations (4.2)-(4.3), we solved for the sensitivity functions and relative sensitivity functions which are shown in Fig. 6 and Fig. 7.

In Fig. 6 concentration $C_P(t;\theta)$ is sensitive to T only for $t < 1$. Also, concentration $C_{A'}(t;\theta)$ is more sensitive to T mostly when $t < 3$. Concentrations $C_L(t;\theta)$ and $C_H(t;\theta)$ appear to be sensitive to T over the whole time interval. None of the concentrations appear to be sensitive to D. However this can be due to the scaling of the parameters. The relative sensitivity functions in Fig. 6 show the sensitivities without these scaling effects.

The relative sensitivity functions in Fig. 7 are more informative for $C_L(t;\theta)$ and $C_H(t;\theta)$. Concentration $C_L(t;\theta)$ seems to be especially relatively sensitive to both parameters when $t \approx 2$. $C_L(t;\theta)$ is somewhat relatively sensitive to D for $t > 2$, but is mostly relatively sensitive to T. Concentration $C_H(t;\theta)$ is more relatively sensitive to T and D as time t increases. Examining Fig. 7 closely, it can be seen that sensitivity to D is non-zero, but all the concentrations are more relatively sensitive to T than they are to D.

4.3 Sensitivity of optimization cost function to D and T

As before, we also calucated the relative sensitivity for the cost function $L(\theta)$ from equation (4.4) for D and T, holding all other parameters fixed. The results of this sensitivity analysis can be found in Table 5. The relative sensitivity value of $L(\theta)$ to T is much greater in magnitude than to D. This corresponds to the results we found in the analysis of concentration sensitivities for the two parameters.

Additionally, we implemented the optimization with the cost function from equation (4.7). The results of this optimization can be found in Table 6. The difference in maginitude between the inital estimate for T and the optimized value is greater than that of D. This result helps to validate the findings of our sensitivity analysis.

In administiring the drug to patients, choosing a good dose time T is more important than the total dose D. Although it's not possible to change T for a bolus input, we can imagine injecting the drug using a drip IV where we do have freedom to change T.

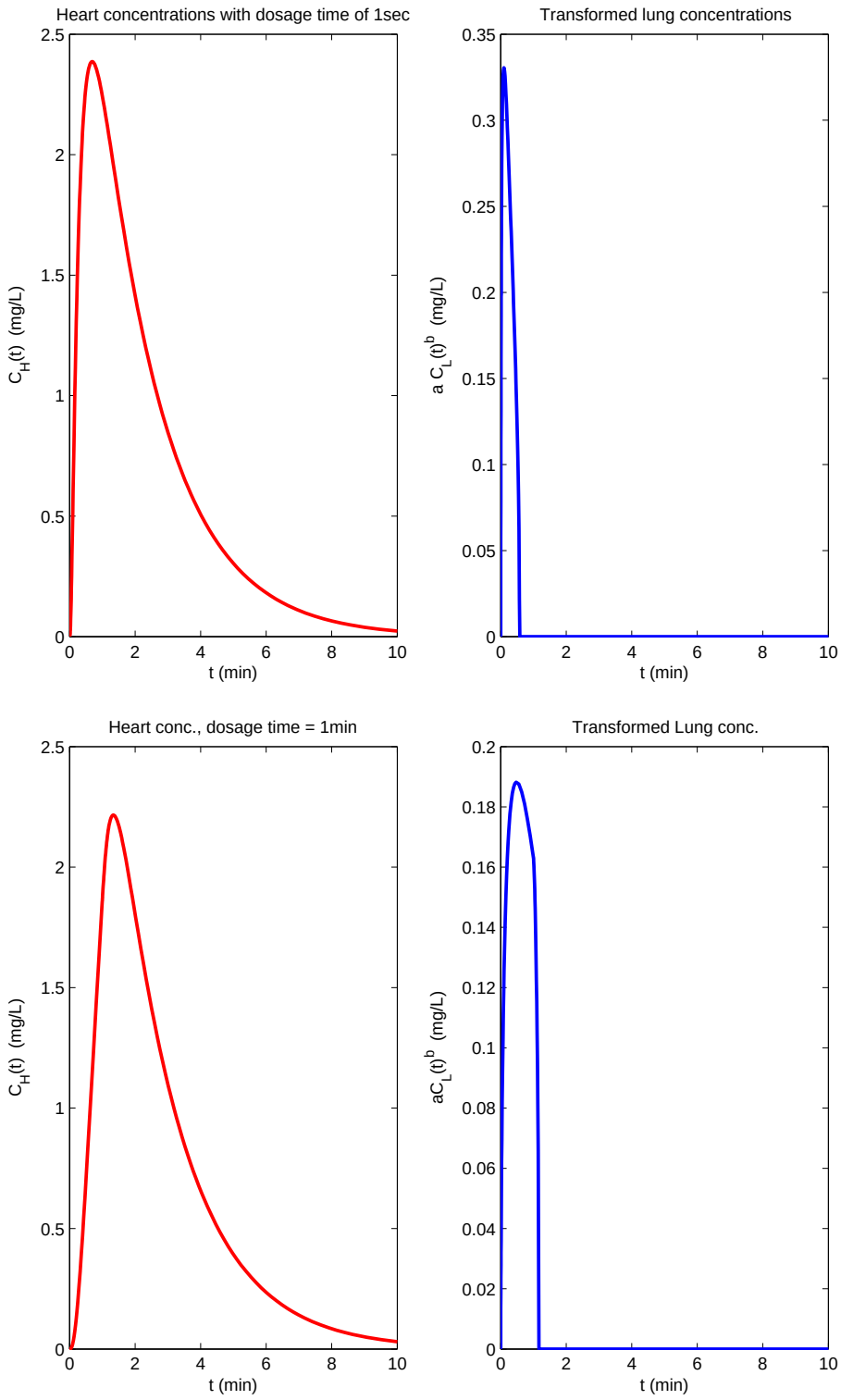

Figure 9: $C_H(t)$ and $aC_L^b(t)$ for T= 1 minute, a=0.11, and b=0.38.

4.4 Optimization with Additional Cost Funtions

It is important to find an optimal dose and injection time with the ultimate goal of determining efficacy. One method to optimize efficacy is to minimize the heart concentration while maximizing the lung concentration. In the earlier section, we saw that among the parameters dosage level D and injection time T the concentrations were more suseptible to change in T over change in D. In this section, we fix a dosage level of 100 mg, say, and

try to find an optimal value for T. For that we set up what are known as cost functions of T and find the value of T that minimizes the cost function. Among the different cost functions considered were:

$$C_1(T) = \frac{\max_t C_H(t;T)}{\max_t C_L(t;T)}, \tag{4.8}$$

$$C_2(T) = \frac{\int_0^{t_1} C_H(t;T)dt}{\int_0^{t_1} C_L(t;T)dt}, \tag{4.9}$$

$$C_3(T) = (\max_t C_L(t;T))^{-1},\ T \in S_3 = \{T :\ \max_t C_H(t;T) \leq C_0\}, \tag{4.10}$$

$$C_4(T) = (\max_t aC_L(t;T)^b)^{-1},\ T \in S_4 = \{T :\ \max_t C_H(t;T) \leq C_0\}. \tag{4.11}$$

Note that for cost function C_1, we choose the dosage time T so as to minimize the ratio of the peak heart and lung concentrations. Empirical evidence suggests that as T increases, both the peaks tend to decrease, so perhaps their ratio may have a minimizer. For the cost C_2, we minimize the ratio of total mass of drug captured in the heart and lung. The upper limit t_1 for the integral is chosen to be the time until which the drug remains in the body. For cost functions C_3 and C_4, we maximize the peak lung concentration such that the heart concentration stays below a given threshold value C_0. For C_4, values of a and b are chosen to transform the graph of the lung concentration over time so that it grows at almost the same rate as that of the heart concentration. Then the new peak is more likely to have a minimizer.

Cost functions C_1 - C_3 returned non-informative results, finding that an infinite dose should be given at an infinitesimal time. This is counter-intuitive to what we expect to find. These results came about because those cost functions were monotonic, so instead we considered the cost function C_4.
For the cost function C_4, we choose $a = 0.11, b = 0.38, C_0 = 2$. We get the values of a and b by minimizing the sum of squares of differences between the heart and transformed lung concentrations when the dosage level $D = 100mg$ and the dosage time $T = 1$ second. Figure 8 shows the plot of heart and transformed lung concentrations over time when $D = 100$ mg and $T = 1$ second. Figure 9 shows the concentration plots when $T = 1$ minute. One can easily see that the shapes of the the heart and transformed lung concentrations do not change much by varying T from 1 second to 1 minute. The optimal dosage time turns out to be 2.22 seconds.

5 Investigation of a Different Dosing Strategy

Typically when a drug is given to a patient through an IV, it is administered at a constant rate.

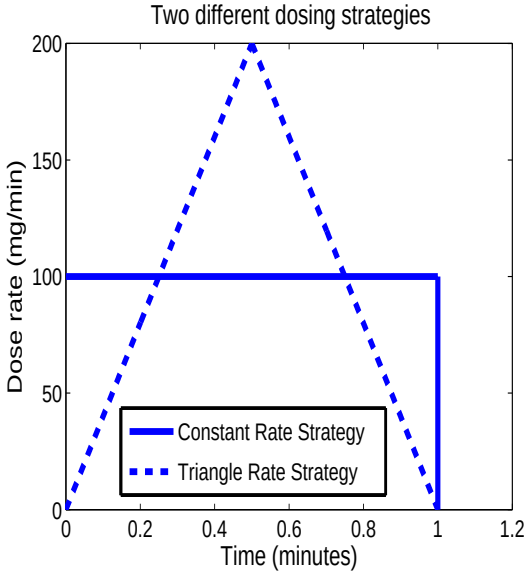

Figure 10: Constant (square wave) and triangle dose rate strategies.

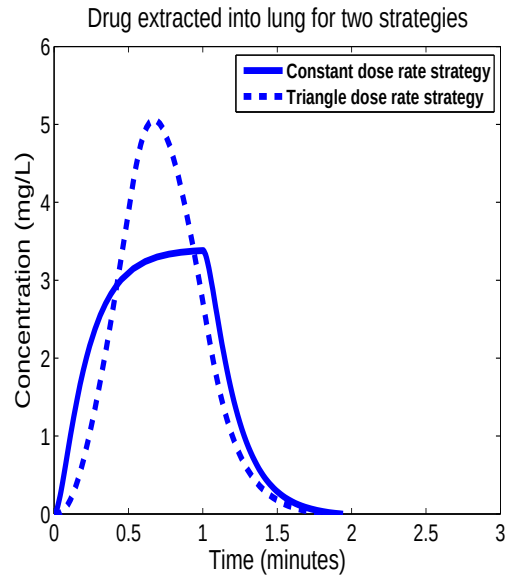

(a)

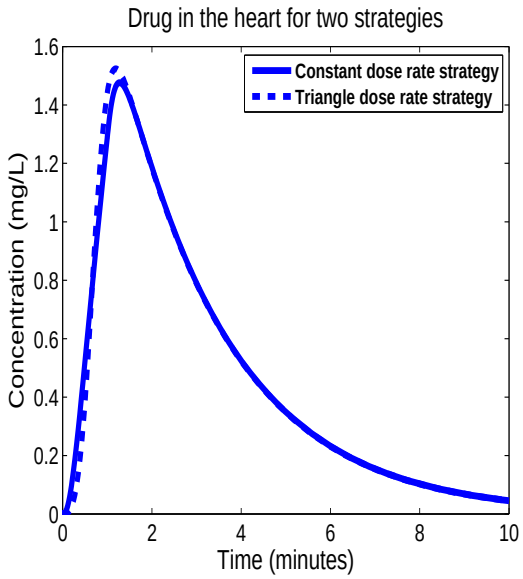

(b)

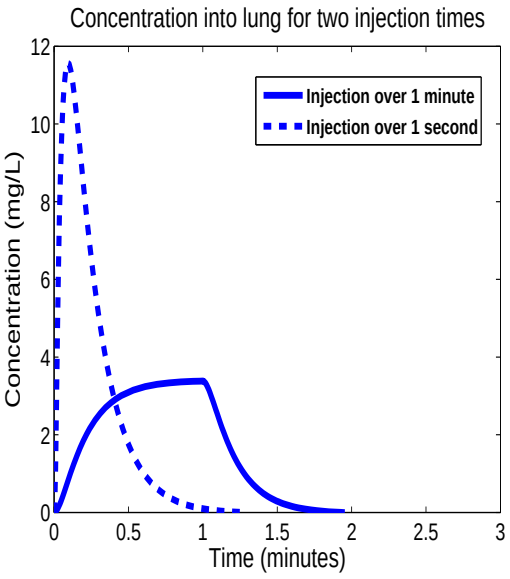

(c)

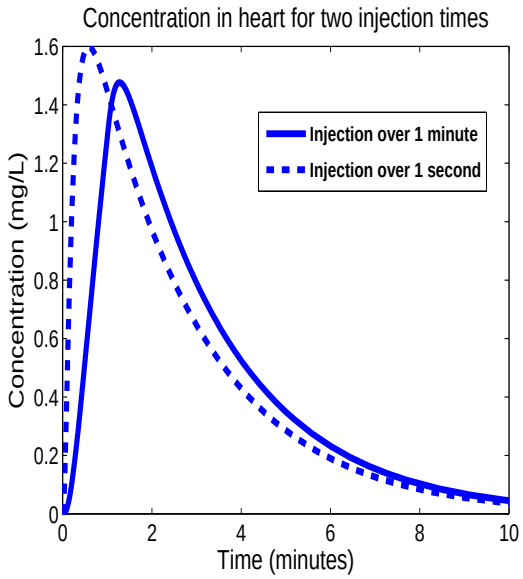

(d)

Figure 11:
(a) Comparison of constant and triangle dose rate strategies for lung.
(b) Comparison of constant and triangle dose rate strategies for heart.
(c) Comparison of 1 minute and 1 second injection times for lung.
(d) Comparison of 1 minute and 1 second injection times for heart.

However, one can imagine different dosing strategies where the rate at which the drug is applied is not constant. For instance, one such strategy (referred to here as the triangle dosing strategy) could be constantly increasing the rate at which the drug is applied until some peak rate is reached and then decreasing the rate back down to zero. In a clinical setting, this would involve a nurse increasing the concentration of the drug in the solution

administered to the patient from zero to a peak concentration and then decreasing the concentration back down to zero. A comparison of two different dosing strategies - the constant and triangle dosing strategies, can be seen in Fig. 10.

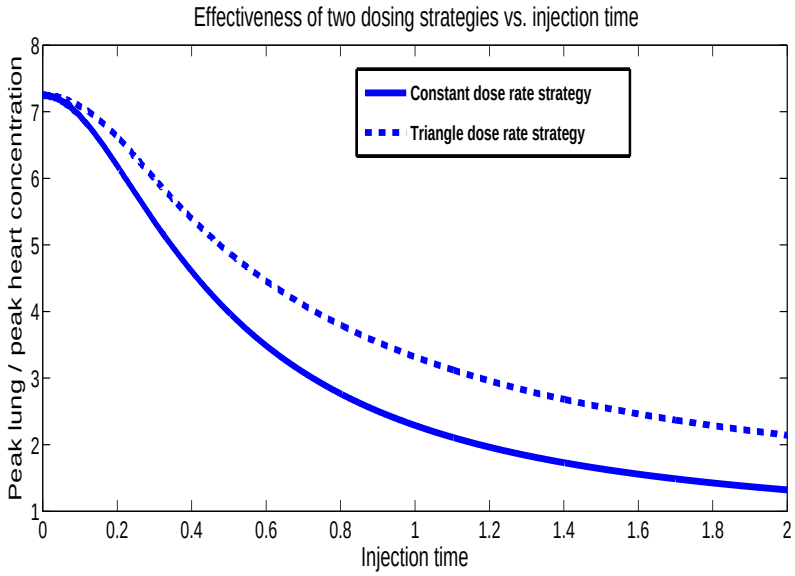

Figure 12: $\frac{max_t C_L(t;\theta)}{max_t C_H(t;\theta)} vs. T.$

Simulations performed with the model predict that dosing strategy does make a difference on peak concentration extracted into the lung for longer intervals of injection time. A comparison of the peak extraction into the lung for the two strategies can be seen in Fig. 11(a) for 1 minute injection intervals. As can be seen in the figure, the peak extraction concentration into the lung is markedly higher when the triangle dosing strategy is applied. In addition, as shown in Fig. 11(b), the peak concentration of the drug in the heart is not sensitive to the dosing strategy. This suggests that one can significantly impact how much drug reaches the lung as compared to the heart for long injection intervals. However, it turns out that the length of the injection interval is much more important for maximizing the ratio of the peak concentration extracted into the lung as compared to the heart and that shorter injection intervals maximize this ratio. This can be summarized in Fig. 11(c) and Fig. 11(d) where one can notice that the peak for the lung curve is significantly higher for an injection interval of 1 second as compared to 1 minute while the peak of the heart curve does not change much. In addition, simulations revealed that dosing strategy does not impact the peaks of either the heart or lung curves for small injection intervals.

The discussion above can all be summarized by Fig. 12. The figure shows that small injection intervals maximize the ratio of peak concentration extracted into the lung to peak concentration in the heart. It is also shown in Fig. 12 there is no difference in this ratio for the two methods over short injection intervals, but that there is a difference for the two methods over longer injection intervals. So, since small injection intervals maximize the ratio of peak lung concentration to peak heart concentration and dosing strategy does not significantly affect this ratio for small injection times, we can conclude that the strategy for injecting the drug is not important for maximizing the ratio of peak concentrations for the heart and lung in the current model.

6 Application of the model to predict erythromycin-induced QT interval prolongation.

Erythromycin is a macrolide antibacterial drug that sometimes causes QT prolongation [7, 22]. The QT interval is a measurement related to the period of an individuals heart beat, and QT prolongation indicates an increased length of the interval [13]. QT prolongation is associated with drug-induced torsades de pointe (TdP) cardiac arrhythmias [7, 12]. The majority of TdP cases occur in women, perhaps reflecting the fact that they naturally

tend to have longer QT intervals than men [7]. Drici, et. al., performed *in vitro experiments* with male and female rabbit hearts perfused by the Langerdorff technique. They measured the QT response to erythromycin at concentrations similar to the plasma concentrations attained during clinical therapy and their results showed a significantly greater QT prolongation in female rabbit hearts [7].

In this section we show how the model can be used to predict erythromycin-induced QT prolongation. First we simulated injection of a single therapeutic dose D of erythromycin administered with constant dose rate D/T. Erythromycin lactobionate is used for intravenous delivery of erythromycin and has a suggested therapeutic dose of about 20 mg/kg/day for humans [8]. We used this same therapeutic dose to determine the total dose D for the simulations, which for a mature 68 kg female sheep resulted in $D = 1360$ mg. The coronary artery supplies blood to the heart muscle and the model compartment C_H corresponds to the coronary sinus which provides the main venous drainage for the coronary artery. Therefore, we made the assumption that the simulated concentration C_H is indicative of the concentration of erythromycin in the heart tissue. We further assume that the perfusion concentrations used by Drici, et.al. [7], that produced the QT prolongation, are equivalent to the coronary sinus concentration C_H. We then used the data for the female rabbit hearts in Fig. 2 of [7], which plots the ratio of the observed QT interval over the baseline value as a function of the erythromycin concentration, to convert from simulated coronary sinus concentration C_H to QT prolongation values using linear interpolation.

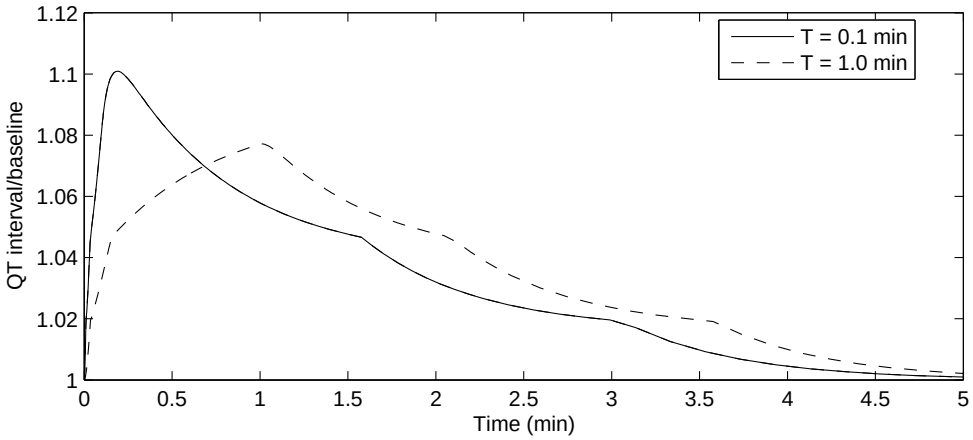

Figure 13: Predicted QT interval prolongation in female sheep as a function of time for a single 1360 mg dose delivered with $T = 0.1$ min (solid line) or $T = 1.0$ min (dashed line).

Figure 13 plots the predicted QT prolongation (increase over baseline) as a function of time for $D = 1360$ mg and $T = 0.1$ min (solid line). From Fig. 13 we can see that as the erythromycin bolus moves through the system the QT interval increases. At the peak erythromycin concentration the QT interval is predicted to be 1.10 times its baseline value. Also plotted in Fig. 13 is the predicted QT prolongation for the same total dose delivered over a longer time $T = 1.0$ min (dashed line). In this case the peak erythromycin concentration is reduced and the maximum QT prolongation is approximately 1.08 times the baseline value. These results show how the model can be used to predict QT prolongation, but requires two assumptions: 1) that there is a direct correspondence between coronary sinus concentration C_H and the experimental perfusion concentrations allowing us to convert from C_H to QT interval prolongation and 2) that the erythromycin-induced QT response in sheep is similar to that in rabbits.

7 Statistical Considerations

At this point we have developed a deterministic model set to the specific initial conditions provided via empirical prior evidence. This allows for a convenient formulation for the maximization of dosage and time of dose administration in a modeling framework. Although designed under the parameters of animal models, the compartments can easily be adapted to represent the human body.

The three most prominent issues that face statisticians when developing pharmacokinetic models include specification of the model structure, the collection of human data, and estimation of the parameters [10]. The

preceding methods section and discussion have dealt extensively with the first of these issues. In the stated model, the desire for a simple model motivates the four compartments used: we model the time-dependent concentrations in the pulmonary artery (following mixing in the bloodstream following injection), absorption into the lung, the concentration in the pulmonary arch, and finally the concentration absorbed into the heart tissue via the coronary artery. It is relevant to note that the model used appears to fit what is known about the drug, but poor model performance could possibly indicate violations of these assumptions.

The parameter values such as lung volume, heart volume, cardiac output, etc., should more appropriately be considered as correlated random variables, with some directly measurable and known, while others are functions of random variables that must be estimated based on observable relationships. Furthermore, the variation of these parameters should have a direct and measurable effect on the concentration of the drug that reaches the target tissues; thus, in a stochastic framework these are more appropriately viewed as covariates in a nonlinear statistical model. Ultimately, it is of interest to describe the changes of drug concentrations in the bloodstream attributable to the various mixing compartments.

Other difficulties with collecting human data are not quite as straightforward, especially regarding the dynamics of a previously unobserved drug's performance in the human body. Relationships and evidence gleaned from animal models do not necessarily translate to humans. Furthermore, there do not exist tissue samples from *in vivo* experiments, and *in vitro* data, if it exists, often does not fully represent the dynamics of a living organ. Ultimately, these are the parameters that need to be estimated, and thus the prior distributions we use should be diffuse, representing our lack of knowledge about the drug in the human body. Furthermore, we assume the timing of the dose is negligible in each compartment, and thus we largely ignore the transit times between compartments. Methods have been proposed to account for this timing, which may contribute to more precise models of concentrations [9].

Finally, even with precise measurements of the dose that eventually reaches the coronary tissue, there is likely inter-individual variability in the probability of an adverse event such as a PVC that cannot be strictly accounted by a deterministic pharmacokinetic model. The proposed model attempts to quantify and ideally develop a balanced dosage strategy that allows the greatest clinical benefit at a minimal risk of adverse events, but the boundary between the hypothetical and the empirical can be quite vast. A stochastic approach could be utilized to account for the uncertainty inherent between dosage administration and observed response.

8 Discrepancies and Future Work

The model constructed has a few shortcomings, for various reasons. One major constraint encountered was the amount of time that was alloted to derive, implement and analyze the results. This led to observeable inconsistencies in the differential equations, but there was not ample time to fix everything. Even so, the results obtained have provided a great deal of insight into how the kinetics in the lung and heart should be modeled. And while many questions remain, some of the important ones have been answered.

Currently the concentrations being modeled show the proper qualitative physical behavior. It has been empirically observed that substances administered into the bloodstream undergo diffusion and advection. The model successfully shows this behavior, as diffusion can be observed by the relative height and position of the drug, and advection is demonstrated by the fact that the concentration moves from one organ to the next.

One of the major issues that is still being investigated is the exact physiological interpretation of C_L in equation (2.16). If the second term in the right hand side (RHS), $\frac{V_0 C_L(t)}{K_m + C_L(t)}$, is dropped, then no metabolism occurs. When this is the case, after taking the anti-derivative of both sides, equation (2.16) simply says that $C_L = E_L C_{A'}$, which indicates that C_L represents the amount of concentration that is extracted into the lung. Now applying the second term in the RHS results in metabolization of this quantity. However, it is incorrect to metabolize the quantity of the lung that is being extracted, which results in a negative concentration for C_L. It is believed then that metabolization in the lung must be taken into account elsewhere, but the appearance and location of such a term in the equations is still unclear.

Another problem that has not been addressed is the time delays experienced from travelling in the vascular system from one organ to the next. This will inherently limit the overall reliability of the resulting concentrations, since it directly affects the peak concentrations observed. Similarly, the model does not account for recirculation of the drug through any target organs, which will affect concentration values at intermediate times. This also means that steady state dose concentrations cannot be established or analyzed.

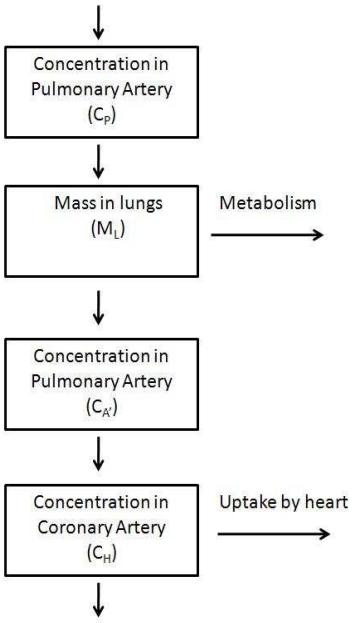

Figure 14: Representation of Model for Future Work.

There are many directions that can be taken in the future for this project. If we were to have more time to work on this project, we would first want to modify the model. After examining the system of equations (2.14) through (2.22), one may notice that the C_L equation is not coupled with the rest of the system. While the system modeled in this paper is represented in Fig. 2(b), the system that we are actually interested in can be shown in Fig. 14. To modify our current system to one in which the C_L compartment is coupled with the rest of the system, the E_L term in equations (2.16) and (2.17), which is currently a constant, should be changed to a function of C_L, i.e. $E_L \equiv E_L(C_L)$. There is in fact evidence that binding and extraction into the lung is saturable, and so it makes sense to make the E_L term a function of C_L [6].

As of now, the interpretation of the lung compartment is a bit confusing. While the C_A, C_P, and C_H compartments represent concentration in blood, the C_L compartment represents concentration in an organ. In general, when a compartment represents an organ, change in mass rather than change in concentration should be modeled [11], and so the next version of the model should incorporate this discrepancy. With our current model, we were unable to establish a therapeutic window for the drug. A therapeutic window can quantify which doses have positive responses, and which doses have negative responses (arrhythmias). Knowledge of a therapeutic window allows for a therapeutic dosage to be established. With the modified model, we would run simulations to determine if a thearepeutic window could be obtained.

It is important to note that the modeling process is iterative and should involve communication and collaboration with experimentalists; this iterative process is summarized in Chapter 1 of [5] and can be seen in Fig. 15. After analysis of our current model, it has become apparent that revisions need to be made. With the next formalization of our model, it would be helpful to obtain experimental data to validate our model and help inform the analysis process. This would allow for comparison of our model with the actual physiological system. If the new model adequately represents that physiological system, the model could be used to design experiments to try to find a therapeutic window. If the model needs further refinement, it could be used to inform experimentalists on the data needed for further model improvement. This type of approach has been taken by Banks et al. in several modeling projects (for example, see [2], [3], and [4]).

In the future, we would also want to validate the modified model with experimental data on the drug. Statistical analysis could be performed to estimate the distribution of the parameters for populations. Another direction we could take in the future would be to examine the oral dosing strategy. Right now the model is specific to the

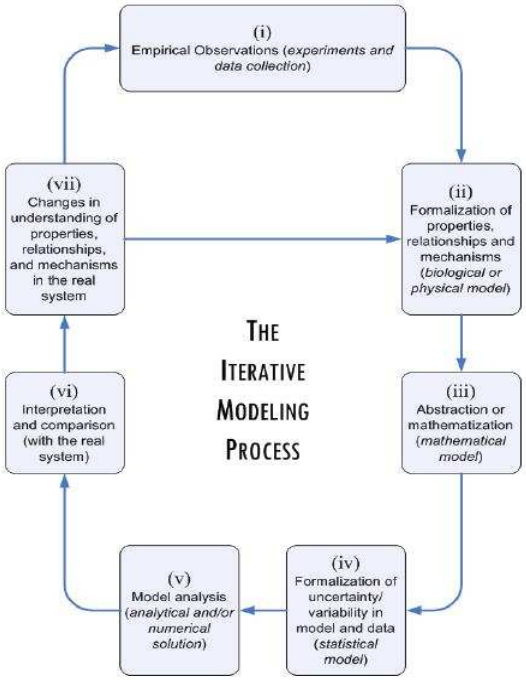

Figure 15: Iterative Modeling Process (figure taken from [5]).

first-pass dynamics of the drug, but it would be interesting to examine the role of the digestive system as well as the liver on the distribution of the drug in the heart and lungs. With this model we would be able to work with researchers to develop experiments to try to find an optimal oral dosing strategy.

9 Acknowledgments

This material was based upon work supported by the Statistical and Applied Mathematical Sciences Institute which is funded by the National Science Foundation under grant number 08-SC-NSF-1025. Any opinions, findings, and conclusions or recommendations expressed in this material are those of the authors and do not necessarily reflect the views of the National Science Foundation.

References

[1] Bai P, Banks HT, Dediu S, Govan AY, Last M, Lloyd AL, Nguyen HK, Olufsen MS, Rempala G, Slenning BD. Stochastic and deterministic models for agricultural production networks. *Mathematical Biosciences and Engineering* 2007; 4(3):373-402

[2] Banks HT, Davidian M, Hu S, Kepler GM, Rosenberg ES. Modeling HIV Immune Response and Validation with Clinical Data. Center for Research in Scientific Computation Technical Report CRSC-TR07-09, NCSU, Raleigh NC. 2007.

[3] Banks HT, Banks JE, Dick LK, Stark JD. Estimation of dynamic rate parameters in insect populations undergoing sublethal exposure to pesticides. *Bulletin of Mathematical Biology* 2007; 69(7): 2139-2180 May, 2005

[4] Banks HT, Bokil VA, Hu S, Dhar AK, Bullis RA, Browdy CL, Allnutt FCT. Modeling shrimp biomass and viral infection for production of biological countermeasures. *Mathematical Biosciences and Engineering* 2006; 3(4): 635-660

[5] Banks HT, Tran HT. *Mathematical and Experimental Modeling of Physical and Biological Processes.* Boca Raton: CRC Press, 2009, to appear.

[6] Cassidy SS, Scharf SM. *Heart-Lung Interactions in Health and Disease.* Danbury: Marcel Dekker Incorporated, 1989.

[7] Drici MD, Knollmann BC, Wang WX, Woosley RL. Cardiac actions of erythromycin - Influence of female sex. *JAMA-Journal Of The American Medical Association* 1998; 280(20):1774-1776

[8] Drugs.com. (July 24, 2008).Erythrocin. Retrieved July 25, 2008, from the World Wide Web: `http://www.drugs.com/pro/erythrocin-injection-usp.html`

[9] Leitnaker, MG. Estimation of delay times in stochastic compartmental models. *Biometrics* 1989; 45,4; 1239-1247

[10] Mezzetti M, Ibrahim JG, Bois FY, Ryan LM, Ngo L, Smith TJ. A bayesian compartmental model for the evaluation of 1,3-butadiene metabolism. *Applied Statistics* 2003; 52(3):291-305

[11] Ottesen JT, Olufsen MS, Larsen JK. *Applied Mathematical Models in Human Physiology.* Washington D.C.: Society for Industrial & Applied Mathematics, 2004.

[12] Owens RC, Nolin TD. Antimicrobial-associated QT interval prolongation: Pointes of interest. *Clinical Infectious Diseases* 2006; 43(12):1603-1611

[13] Noble A, Johnson R, Thomas A, Bass P. *The Cardiovascular System.* New York: Churchill Livingstone, 2005.

[14] Upton RN. A model of the first pass passage of drugs from i.v. injection site to the heart—parameter estimates for lignocaine in the sheep. *British Journal of Anaethesia* 1996; 77: 764-772

[15] Upton RN, Ludbrook GL. A physiological model of induction of anaesthesia with propofol in sheep.1.Structure and estimation of variables. *British Journal of Anaethesia* 1997; 79:497-504

[16] Upton RN, Ludbrook GL. A physiologically based, recirculatory model of the kinetics and dynamics of propofol in man. *Anesthesiology* 2005; 103:344-352

[17] Upton RN. Relationships between steady state blood concentrations and cardiac output during intravenous infusions. *Biopharmaceutics & Drug Disposition* 2000; 21:69-76

[18] Upton RN, Ludbrook GL, Grant C, Martinez AM, Sci DM. Cardiac output is a determinant of the initial concentrations of propofol after short-infusion administration. *Anesth Analg* 1999; 89: 545-52

[19] Upton RN. A recirculatory basis for pharmacokinetics and pharmacodynamics - a tutorial for anaesthetists. `http://www.anaesthesia.adelaide.edu.au/~richard/tutorial/index.html`

[20] Upton RN, Doolette DJ. Kinetic aspects of drug disposition in the lungs. *Clinical and Experimental Pharmacology and Physiology* 1999; 26: 381-91

[21] Wetherington J. Personal communication, July 21, 2008.

[22] Wisialowski T, Crimin K, Engtrakul J, O'Donnell J, Fermini B, Fossa AA. Differentiation of arrhythmia risk of the antibacterials moxifloxacin, erythromycin, and telithromycin based on analysis of monophasic action potential duration alternans and cardiac instability. *Journal of Pharmacology and Experimental Therapeutics* 2006; 318(1):352-359